■ Hydrofluorination |*Hot Paper*|

A HF Loaded Lewis-Acidic Aluminium Chlorofluoride for Hydrofluorination Reactions

Maëva-Charlotte Kervarec,[a] Erhard Kemnitz,[a] Gudrun Scholz,[a] Svemir Rudić,[c] Thomas Braun,*[a] Christian Jäger,[b] Adam A. L. Michalchuk,[b] and Franziska Emmerling[b]

Abstract: The very strong Lewis acid aluminium chlorofluoride (ACF) was loaded with anhydrous HF. The interaction between the surface of the catalyst and HF was investigated using a variety of characterization methods, which revealed the formation of polyfluorides. Moreover, the reactivity of the HF-loaded ACF towards the hydrofluorination of alkynes was studied.

Introduction

Fluorinated building blocks are of high interest, due to the often drastic change in properties of fluorinated compounds, when compared to their non-fluorinated analogues.[1,2] Correspondingly, many studies focus on the incorporation of a fluorine atom into organic molecules.[3–7] New pathways are being developed to achieve the formation of C—F bonds, which is of high interest in materials science, pharmaceuticals, and agrochemicals.[6–8]

Aluminium fluoride-based catalysts can be considered as the strongest solid Lewis acids known.[9–11] Among them, aluminium chlorofluoride (ACF, $AlCl_xF_{3-x}$, $x = 0.05–0.3$, patented by Dupont) is of high interest, in part because of its large surface area and high Lewis acidity, which is comparable to the one of SbF_5.[12,13] Its properties and reactivity have been intensely investigated, showing that a variety of reactions can be mediated.[13–26] For instance, H/D or Cl/F exchange reactions were reported at ACF.[20,23,27–29] In the presence of a hydrogen source, such as triethylsilane and triethylgermane, hydrodehalogenation, or dehydrohalogenation of C—F bonds or C—Cl bonds

were achieved.[16,17,26,30] In the additional presence of benzene, Friedel–Crafts products can be generated when using Et_3SiH as a hydrogen source. However, when the reactions were performed in C_6D_{12} without the addition of any Et_3SiH, 1-fluoropentane was converted into traces of 2-fluoropentane and 3-fluoropentane, which might be formed by dehydrofluorination and a subsequent HF addition to the double bond of 2-pentene.[17]

The interaction of $HSiEt_3$ or $HGeEt_3$ with the surface of ACF was studied in some detail.[17,24] Pulse TA evidenced the presence of a strong interaction of the adsorbed silane or germane at the surface. MAS-NMR spectroscopy revealed a considerable difference between the two materials. The data suggested an interaction of the silanes at the surface, which might lead to a silylium-like character of the silicon-containing species. For the germanes, two distinct types of surface-bonded germane species were detected.[17] An interaction of HF with β-AlF_3 was studied in 2007 using DFT calculations. The investigation reveals a protonation of basic fluoride centers at the surface to yield a polyfluoride-like structure, which can also interact with undercoordinated Al sites.[31] In another study, aluminium alkoxide fluoride $[AlF_{2.7}(OR)_{0.3}]$ was treated with gaseous HF at $100\,°C$ or $200\,°C$, resulting in the formation of an amorphous AlF_3 phase with low surface area ($100\ m^2g^{-1}$) which presumably contains surface-immobilized HF.[32]

This work covers studies on the properties of HF-loaded ACF. Surface and bulk characterization methods were used to investigate the interaction of HF with the surface and the influence on the bulk. The hydrofluorination of alkynes led to the formation of hydrofluoroolefins (HFOs).

[a] M.-C. Kervarec, Prof. Dr. E. Kemnitz, Priv.-Doz. Dr. G. Scholz,
Prof. Dr. T. Braun
Department of Chemistry, Humboldt-Universität zu Berlin
Brook-Taylor-Straße 2, 12489 Berlin (Germany)
E-mail: thomas.braun@cms.hu-berlin.de

[b] Prof. Dr. C. Jäger, Dr. A. L. Michalchuk, Priv.-Doz. Dr. F. Emmerling
BAM Federal Institute for Materials Research and Testing
Richard-Willstätter-Straße 12489 Berlin (Germany)

[c] Dr. S. Rudić
ISIS Neutron and Muon Source, STFC
Rutherford Appleton Laboratory, Chilton, Didcot (UK)

Supporting information and the ORCID identification number(s) for the author(s) of this article can be found under:
https://doi.org/10.1002/chem.202001627.

Results and Discussion

Synthesis of HF-loaded-ACF

Freshly dried HF was condensed (8 wt. %) onto a defined amount of ACF. A slight change in color was observed from yellowish to brown-yellow. After that, a vacuum was applied

Chemistry–A European Journal

Full Paper
doi.org/10.1002/chem.202001627

Chemistry Europe
European Chemical
Societies Publishing

for 15 minutes to remove any excess of HF, which did not interact with the surface.

MAS NMR Spectroscopy

The ^{27}Al MAS NMR spectra shown in Figure 1 exhibit signals at $\delta = -16$ ppm for both ACF and the HF-loaded ACF samples. The chemical shift is typical for ACF containing AlF_6 units and a few $AlCl_xF_{6-x}$ units.[14] However, the ^{27}Al NMR signal of the HF-loaded ACF appears more narrow, with a line-width decrease of about 250 Hz, which presumably indicates a slightly better-ordered aluminium fluoride matrix as a consequence of HF loading.

Figure 2 shows the ^1H MAS NMR spectrum for the ACF sample loaded with HF. Four different signals can be distinguished (see also Figure 6 below). The signal for HF-loaded ACF at $\delta = 17$ ppm is typical for strongly bridged HF units and is in good agreement with the values reported for FHF^- moieties.[33,34] The signal at $\delta = 11$ ppm is as well compatible with the literature, suggesting the presence of $[F(HF)_n]^-$ moieties at the surface of ACF.[33] Signals for solution spectra of tetrabutylammonium $[F(HF)_3]^-$ salts appear at $\delta = 11.8$ ppm and the FHF^- anion results in resonance at $\delta = 16.1$ ppm.[33] The broad feature at $\delta = 6$ ppm for the HF-loaded ACF is different in line width and shape and includes at least two signals, which could
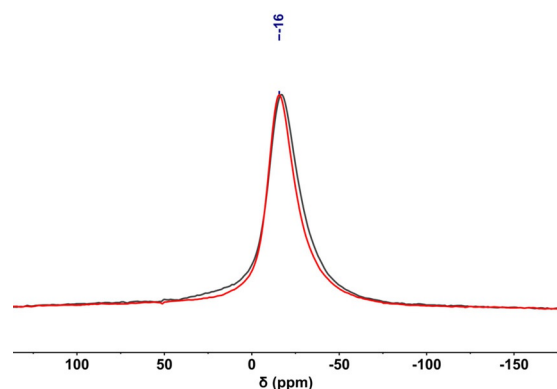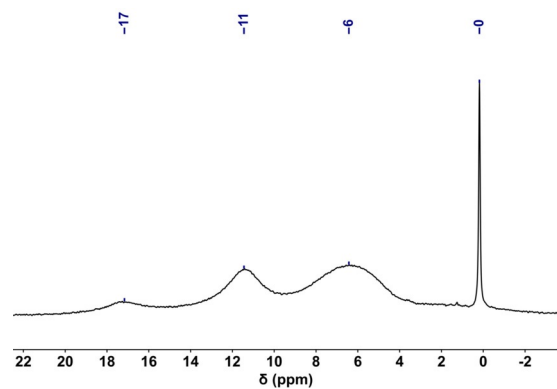
be assigned to larger polyfluoride clusters, including the possibility of a second layer of HF.[33,34] We cannot entirely exclude the presence of some adsorbed water molecules, despite careful handling during the sample preparation, because the resonance at $\delta = 6$ ppm is also typical for them (see also below).[35,36] The narrow signal at $\delta = 0$ ppm is typical for highly mobile species, and might, therefore, be attributed to physisorbed HF. Scheme 1 shows schematically four possible interactions of HF with the surface of ACF, assigned to their corresponding signals observed in the ^1H spectra.

The ^{19}F NMR MAS NMR spectra of HF-loaded ACF and ACF are depicted in Figure 3. Both samples show a broad asymmetric signal, which is caused by the fluorides in the bulk of ACF.[37,14] Noticeably, the maximum of the peak is shifted from $\delta = -165$ ppm (ACF) to $\delta = -167$ ppm (HF-loaded ACF), along with a diminished line width of about 3 kHz, again indicating a slight reorganization of the bulk structure in HF-loaded ACF, which is in accordance with the ^{27}Al MAS NMR spectra. Moreover, the signals are shifted towards the signals observed for crystalline α-AlF_3 or β-AlF_3, which appear at $\delta = -172$ ppm.[37] All signals for the additional fluorine sites due to $[F(HF)_n]^-$ anions can be expected in the same range and are covered by the broad network signal at $\delta = -167$ ppm.[33,34] It should be noted that signals of solution ^{19}F NMR spectra of polyfluoride anions $[F(HF)_3]^-$ in p-toluidinium salts appear at $\delta = -147.2$ and $\delta = -185.0$ ppm, whereas the FHF^- anion shows a signal at $\delta = -155.4$ ppm.[14,37,38] The sharp signal at $\delta = -135$ ppm for the HF-loaded ACF sample corresponds to some physisorbed HF and can be associated with the narrow resonance at $\delta = 0$ ppm in the ^1H NMR spectrum (Figure 2). Figure 4 displays the ^{19}F MAS NMR spin echo spectra for ACF and HF-loaded

Figure 1. ^{27}Al MAS NMR spectra of ACF (black) and HF-loaded ACF (red) measured at 27.5 kHz rotation frequency.
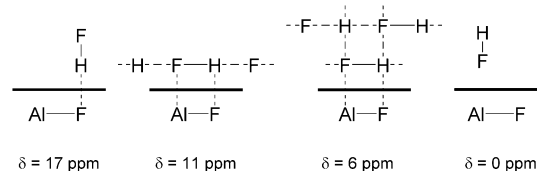
Scheme 1. Schematic representation of possible interactions of HF with the surface of ACF along with the corresponding ^1H chemical shift values.

Figure 2. ^1H MAS NMR spectrum of HF-loaded ACF measured at 27.5 kHz rotation frequency.
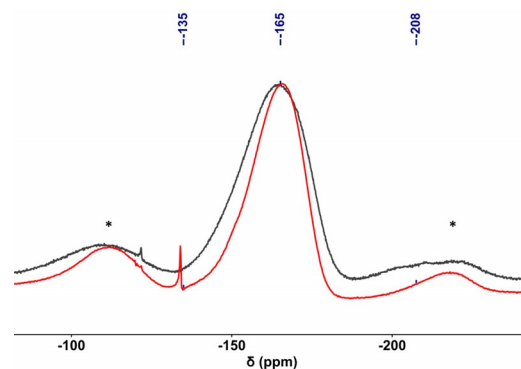
Figure 3. ^{19}F MAS NMR spectra of ACF (black) and HF-loaded ACF (red) measured at 27.5 kHz rotation frequency. Asterisks (*) represent spinning sidebands.
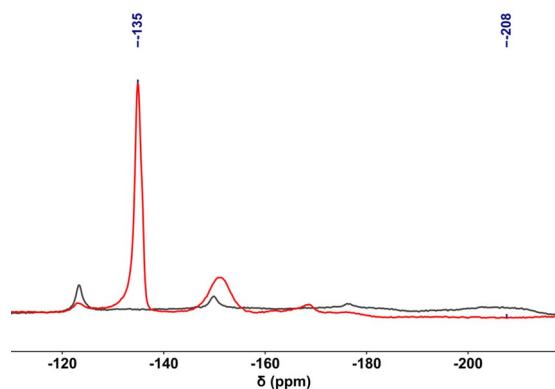
Chemistry–A European Journal

Full Paper
doi.org/10.1002/chem.202001627

Chemistry Europe
European Chemical
Societies Publishing

Figure 4. ^{19}F rotor synchronized spin-echo MAS NMR spectra of ACF (black) and HF-loaded ACF (red) measured at 27.5 kHz rotation frequency.
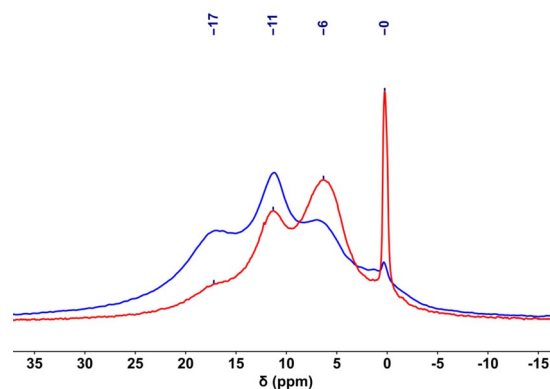

Figure 6. ^{1}H MAS NMR spectrum of HF-loaded ACF (red) and HF-loaded ACF synthesized using less HF (blue) measured at 20 kHz rotation frequency.

ACF. The signal that can be assigned to terminal fluorine atoms bound at aluminium at $\delta = -208$ ppm for ACF does not appear for the loaded sample, suggesting that those terminal fluorine atoms are not present anymore.

In order to verify the presence of physisorbed HF, another batch of HF-loaded ACF was synthesized in the same way as described earlier, only using distinctly less HF. As a consequence, a decrease of both ^{19}F NMR ($\delta = -135$ ppm) and ^{1}H NMR ($\delta = 0$ ppm) signal intensities was observed, supporting the assumption that both signals correspond to physisorbed HF (Figure 5 and Figure 6). Moreover, partial removal of chemisorbed HF was observed as well, clearly visible by the reduced intensity of the signal at $\delta = -167$ ppm in the ^{19}F NMR spectrum as well as the signal at $\delta = 6$ ppm in the ^{1}H NMR spectrum. This indicates a diminished second layer of polyfluoride cluster when less HF is used during the loading of ACF.

Additionally, when the sample loaded with a lot of HF was put under vacuum for 24 hours or heated, a drastic decrease in intensity in the ^{19}F MAS NMR of the bulk signal at $\delta = -167$ ppm was observed, indicating a removal of HF from the polyfluoride network (see Supporting Information, Figure S2). The same trend was observed in the ^{1}H MAS NMR (Supporting Information, Figure S1), where all the signals were reduced, although the one at $\delta = 6$ ppm seems to be less diminished.
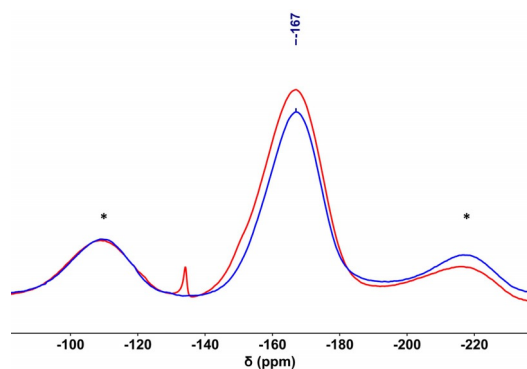
A ^{1}H DQ MAS NMR experiment was performed for the sample loaded with HF (Figure 7). Diagonal and off-diagonal peaks reveal correlations of the signals at $\delta = 6$ ppm and $\delta = 11$ ppm. The signal at $\delta = 17$ ppm does not show any cross peak in the ^{1}H DQ experiment, which indicates the isolated character of the strongly bridged HF with the surface of ACF. A ^{1}H–^{19}F MAS NMR rotor-synchronized correlation spectrum (Figure 8) shows cross-peaks of all proton signals with the signal at $\delta = -167$ ppm for the fluoride bulk, which is superimposed by the ^{19}F signals of the polyfluoride anions $[F(HF)_n]^-$. No correlation was observed between the signal at $\delta = -135$ ppm in the ^{19}F MAS NMR spectrum and the one at $\delta = 0$ ppm in the ^{1}H MAS NMR spectrum, probably due to the high mobility of the physisorbed HF.

With the aim to estimate a conceivable change of the chlorine content in the sample loaded with HF, a ^{19}F–^{35}Cl TRAPDOR NMR experiment was carried out, and the spectra for ACF and the HF-loaded ACF are depicted in Figure 9. The spectra are unique and reveal the presence of chlorine atoms in the network of ACF and HF-loaded ACF. The experiments were performed under the same experimental conditions (completely filled rotors, same masses of the catalysts, the same number of accumulations), and both samples showed signals with comparable peak areas, which indicates that there is no distinct change in the chlorine content after loading with HF.

Figure 5. ^{19}F MAS NMR spectra of HF-loaded ACF (red) and HF-loaded ACF synthesized using less HF (blue) measured at 20 kHz rotation frequency. Asterisks (*) represent spinning sidebands.
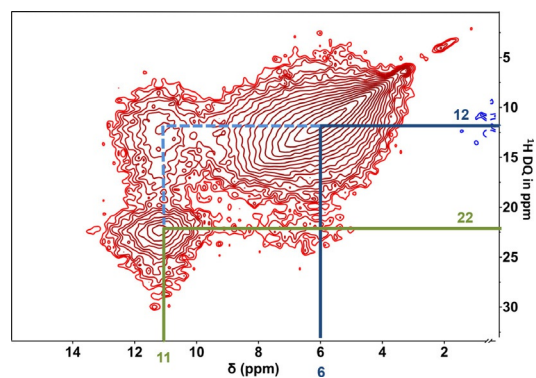

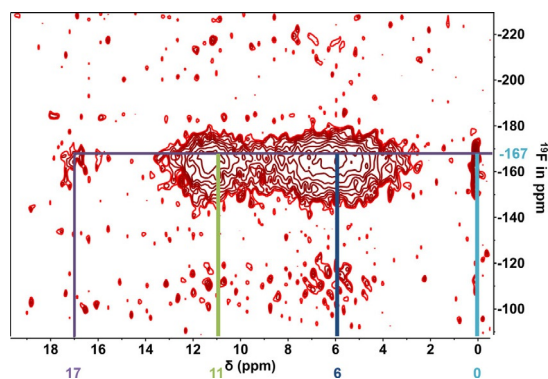**Figure 7.** ^{1}H DQ MAS NMR spectrum of HF-loaded ACF measured at 27.5 kHz rotation frequency.

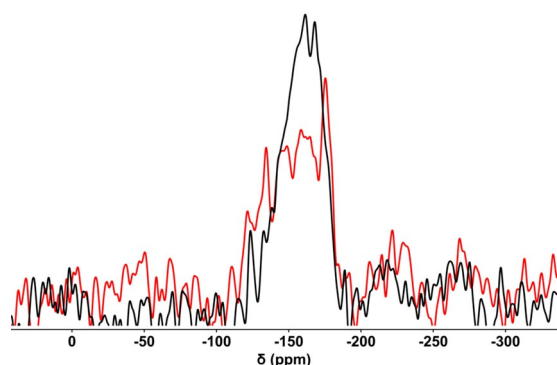**Figure 8.** ^1H–^{19}F MAS NMR correlation spectrum for HF-loaded ACF measured at 27.5 kHz rotation frequency.

Figure 10. FTIR spectra of ACF (black), HF-loaded ACF (red), HF-loaded ACF 200 °C (green) and HF-loaded ACF 400 °C (blue).

Figure 9. ^{19}F–^{35}Cl TRAPDOR MAS NMR spectra of ACF (black) and HF-loaded ACF (red) measured at 27.5 kHz rotation frequency.

FTIR-ATR and INS

The FTIR spectrum shows four broad bands for the HF-loaded ACF sample (Figure 10) with maxima at 1665 cm^{-1}, 1180 cm^{-1}, 1050 cm^{-1}, and 590 cm^{-1}. All those bands are compatible with data for $[F(HF)_n]^-$ anions in p-toluidinium hydrogen difluoride.[39] The band at 1665 cm^{-1} is in the range of the stretching vibrations of $[F(HF)]^-$ anions and the bands at 1180 cm^{-1} and 1050 cm^{-1} relate to bending modes of the $[F(HF)_n]^-$ anions.[39] Likewise, the band at 590 cm^{-1} can be associated with a F-Al-F vibrational mode.[40] Those values are also consistent with a DFT study on the adsorption of HF at a β-AlF$_3$ surface, which imparts different frequency vibrational modes of FHF$^-$ moieties, depending on the binding mode at the respective under-coordinated Al sites.[31] With a half monolayer coverage at a T1 termination, which relates to under-coordinated Al moieties at a (100) surface, the stretching frequency of adsorbed HF giving FHF$^-$ moieties would then be 1654 cm^{-1}, whereas at full monolayer coverage the HF stretch frequency would appear at 1211 cm^{-1}.[31]

For a sample of HF-loaded ACF, which was heated at 200 °C for 4 hours, the signals appear (green spectrum in Figure 10) at the same wavenumbers as for the sample, which did not undergo thermal treatment, however, they are narrower. This suggests desorption of HF by heating the sample, and the observation is in good agreement with the MAS NMR study, which
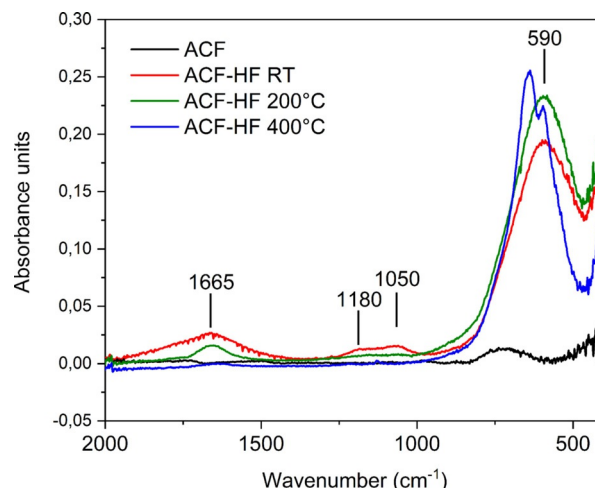
also indicated the presence of less HF after heating (see above). A spectrum of another sample treated at 400 °C was as well recorded, and it showed only typical vibrational modes of the β-AlF$_3$ phase at 596 cm^{-1} and 650 cm^{-1}, which correspond to the stretching and bending mode vibration of F-Al-F moieties, respectively.[37, 40] Previous studies for ACF did not reveal any distinct bands, due to its amorphous character.[13, 14]

To explore further the vibrational spectra of HF-loaded ACF, inelastic neutron scattering (INS) spectra were collected for both the pure and HF-loaded ACF materials (Figure 11). Due to the large incoherent scattering cross-section of hydrogen atoms as compared with aluminium, chlorine, and fluorine atoms, the INS signal of HF-loaded ACF is dominated (albeit not exclusively) by H-containing vibrational modes. This is confirmed by noting the absence of INS features in the pure ACF spectrum (Figure 11, black). The INS spectrum of the HF-loaded material exhibits six vibrational bands: 658 cm^{-1}, 1078 cm^{-1}, 1192 cm^{-1}, 1344 cm^{-1}, 1680 cm^{-1} and approximately 2292 cm^{-1}. These vibrational frequencies are consistent with those obtained by FTIR spectroscopy (Figure 10), but are consistently blue shifted. This contrasts the established trend for HF upon cooling, in which the stronger H···F hydrogen bonding interactions at low temperatures are accompanied by red-shifted vibrational frequencies.[41] An alternative explanation for this blueshift may reside in the chain length (n) or geometry of $[F(HF)_n]^-$ clusters, both of which vary with temperature. Ab initio calculations have suggested that $(HF)_n$ vibrational frequencies vary semi-continuously with chain length.[42] Moreover, similar calculations have demonstrated that cluster geometries influence significantly on vibrational frequencies.[43] Dedicated investigations into the thermal stability of $[F(HF)_n]^-$ clusters upon cooling on ACF surfaces are needed. Additional to the blueshifted frequencies, the INS spectrum suggests the existence of an additional vibrational band at 1344 cm^{-1} which is not visible in the FTIR spectrum.[31] The vibrational band at 2292 cm^{-1} observed in the INS spectrum is consistent with previously reported combination bands observed by IR spectroscopy.[44, 45]

Chemistry–A European Journal

Full Paper
doi.org/10.1002/chem.202001627

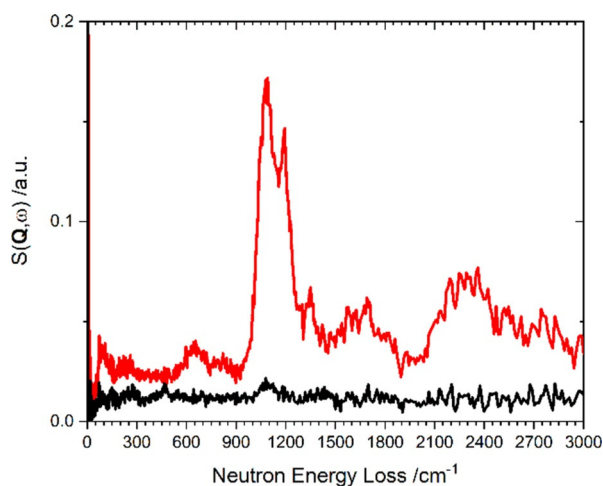**Chemistry Europe**
European Chemical
Societies Publishing

Figure 11. INS spectrum of ACF (black) and HF-loaded ACF (red). In both cases, the low frequency coherent inelastic scattering from the Al sample holder has been subtracted.

Noting the potential for contamination of ACF surfaces with water, we additionally compare the INS spectra of ACF and HF-ACF with that of ice I_h (see Supporting Information, Figure S3). The clear absence of features in the INS spectrum strongly suggests no water is present in the pure phase of ACF. Similarities between the INS spectrum of I_h and HF-ACF are visible. Further analysis of relative scattering intensities does not, however, suggest these similarities to result from the presence of ice I_h on the HF-ACF surface. The lack of water supports the aforementioned NMR results.

Thermoanalysis

The thermal behavior of ACF was studied in the past.[13,14] Differential thermal analysis (DTA) shows at approximately 400 °C a decomposition into gaseous $AlCl_3$ and crystalline phases of AlF_3 (η-AlF_3, θ-AlF_3, and β-AlF_3).[13,14] In contrast, the DTA of HF-loaded ACF displays a continuous exothermic phase transition between 50 °C and 500 °C. Indeed, during the heating time, HF is released from the surface, as indicated by mass spectrometry, and it might fluorinate the catalyst continuously.[46–48] The thermal behavior resembles the one of aluminium alkoxide fluoride, which was treated with diluted gaseous HF.[32] The material also shows a broad desorption range for HF, with a maximum at 200 °C. It is also known that for surfaces covered with adsorbed species compared to uncovered surfaces, the exothermic DTA curve has a larger slope. Indeed, the DTA is extended to a wider temperature range. The TG shows two mass losses around 200 °C and 400 °C, which correspond to a release of HF and a slow fluorination and crystallization process. A total mass loss of about 17 % while heating from room temperature to 500 °C was observed (Figure 12), whereas a 10 % mass loss is detected for unloaded ACF under the same conditions. This indicates that the mass loss related to the release of HF has a maximum of 8 %.
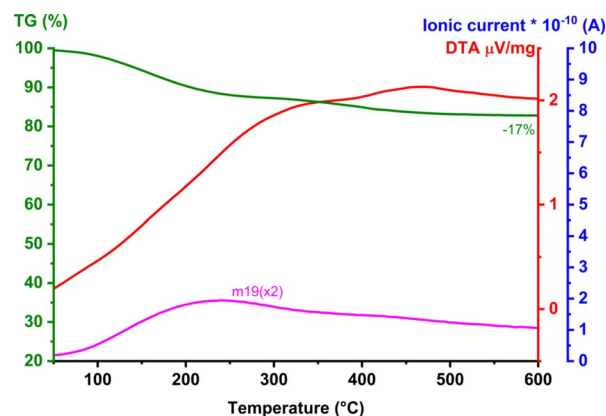

Figure 12. TA-MS curves for HF-loaded ACF; m19 corresponds to HF.

XRD

In order to get a better understanding of the thermal behavior of the samples, powder XRD data were recorded for ACF, HF-loaded ACF, as well as for two HF-loaded ACF samples (Figure 13), which were heated at 200 °C and 400 °C for thirty minutes. In the case of HF-loaded ACF, the diffractogram reveals the presence of an amorphous material, with a very slight crystalline character. This result is consistent with the observation of the MAS NMR studies, which indicate a slightly better-ordered aluminium fluoride (see above). The diffractogram of the heated sample at 200 °C does not differ from the room temperature one, but the one heated at 400 °C indicates the presence of a crystalline β-AlF_3 phase.[37,49]

It should be noted that this behavior is slightly different from the one for pure ACF. When the amorphous material was heated to 400 °C, η-AlF_3 was obtained.[13,14] When the temperature was increased to 500 °C, the Θ-AlF_3 phase was formed, and finally, at 600 °C, the β-AlF_3 phase was observed.[13] This difference can be explained by the fact that in the case of the loaded sample, HF is immediately released and also might fluorinate part of the bulk, which will cause the release of HCl, much faster than it might occur for ACF.
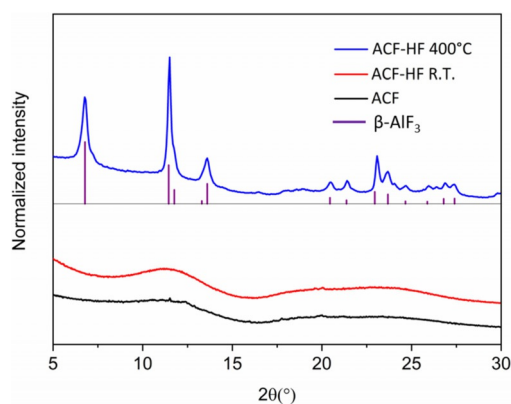

Figure 13. Powder XRD pattern of ACF (black), HF-loaded ACF rt (red), HF-loaded ACF 400 °C (blue) and β-AlF_3 (purple).

Chemistry Europe
European Chemical
Societies Publishing

Surface area determination and pore size analysis

To get information on the morphology properties of the HF-loaded ACF sample, nitrogen sorption studies were performed without any initial degassing process by heating or applying vacuum (Figure 14). According to the isotherm curve, they revealed a low intensity of adsorbed N_2, reaching only 30.5 $cm^3 g^{-1}$ when compared to 99 $cm^3 g^{-1}$ of adsorbed N_2 for ACF. Noticeably, the loaded sample adsorb and desorb much less than ACF; thus, ACF has a very fast adsorption till 0.1 in relative pressure, with a high adsorption value (70 $cm^3 g^{-1}$) and then reaches the maximum value (99 $cm^3 g^{-1}$) slowly. Both ACF and the loaded ACF exhibit a type I isotherm, which indicates a microporosity according to the BET model. The surface area calculated by the BET model showed a smaller value for the loaded sample. This is probably because the pores are filled by HF, leaving low capacity for the N_2 to adsorb. This diminished surface area was as well observed in the case of HF-loaded aluminium alkoxide fluoride, however, the sample was less affected, and a value of 100 $m^2 g^{-1}$ was obtained.[32] The re-determined value for the pure ACF is in accordance with previous studies determined by the BET method (Table 1).[13,19] These observations are confirmed by studies on the pore size distribution using non-local density functional theory (NLDFT), where two distinct kinds of pores for ACF were identified (Figure 15). The studies reveal only one kind of pores for the loaded sample with HF with a diameter range between 14–17 Å. For ACF, micropores of two different sizes were distinguished: one with a diameter of about 12 Å, and another type with a diameter of 20 Å. The results are summarized in Table 1. This might
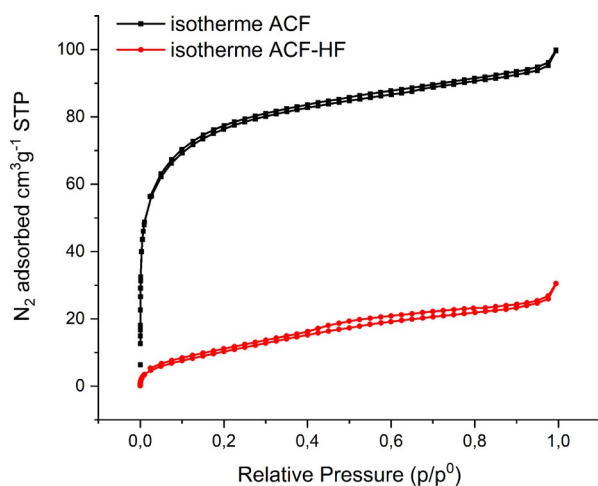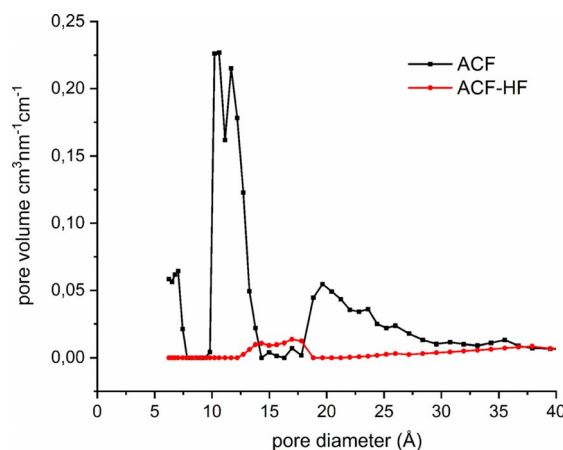

Figure 15. Pore size distribution of the two materials determined by NLDFT.

indicate a complete filling of the smaller pores by HF, with an additional partial filling of the bigger pores, which are present on ACF, hence being reduced in size in the loaded sample. X-ray data on polyfluoride anions in KHF_2 revealed an F-H-F distance of about 2.277 ± 0.006 Å.[45,50] Data for larger anions were also reported such as for $H_4F_5^-$, which reach an F-H-F distance of 2.453 ± 0.002 Å.[51,52]

Deuterated acetonitrile and pyridine-adsorption studied by DRIFTS

Diffuse reflectance infrared Fourier transform spectroscopy (DRIFTS) studies on the adsorption of deuterated acetonitrile were performed on HF-loaded ACF and ACF itself (see Supporting Information, Figure S4). A band of low intensity with a shift of about 67 cm^{-1} to higher energy was detected for the C≡N vibration for the HF-loaded ACF sample (see Supporting Information, Table S1). This large shift indicates that free Lewis acidic sites are still present on the HF-loaded ACF, but in a very small amount. They are as strong as found for ACF since an absorption band with the same energy was found for the surface-bound deuterated acetonitrile.[19] However, the intensity of the bands is much lower for the HF-loaded ACF sample than for ACF, which is in good agreement with the assumption that most of the sites are blocked by HF. Additionally, pyridine was as well adsorbed on the surface of HF-loaded ACF. Two bands with low-intensity at 1540 cm^{-1} and 1490 cm^{-1} indicate the presence of Brønsted-acidic sites, but there is no indication for Lewis-acidity (see Supporting Information, Figure S5).[53–55] Again, in the case of HF-loaded aluminium alkoxide fluoride, when photoacoustic IR of adsorbed pyridine on the surface was performed, the band for the Lewis acid sites was hardly detected.[32] However, in this case, the Lewis acidity could be recovered by desorbing the HF at 350 °C in the presence of dichlorodifluoromethane (R12).[32]

Reactivity

Various reports demonstrate catalytic hydrofluorination reactions of alkynes, using transition metal complexes and different

Figure 14. N_2 sorption isotherm of ACF (black) and HF-loaded ACF (red).

Table 1. Surface area and pore size distribution of ACF and HF-loaded ACF

Material	Surface area by BET [$m^2 g^{-1}$]	Pore size [Å]	Pore volume [$cm^3 g^{-1}$]
ACF	215	12 and 20	0.022 and 0.05
ACF–HF	44	14-17	0.01

Chemistry–A European Journal

Full Paper
doi.org/10.1002/chem.202001627

Chemistry Europe
European Chemical
Societies Publishing

HF sources.[56–62] HF sources including adducts such as DMPU/ HF, Et$_3$N·3 HF, and pyridine·(HF)$_x$ have been used for fluorination, as for instance, demonstrated by Olah in the hydrofluorination of alkynes using pyridinium poly(hydrogenfluoride).[59,62–65] At 0 °C, more than 70 % yield of the corresponding Markownikow alkyl fluorides as products were obtained. Recently, many research groups focus on gold-based catalysts in combination with HF-sources to develop hydrofluorination processes of alkynes.[56,66,67] Indeed, the groups of Nolan, Toste, Miller, and Sadighi, used Et$_3$HF·3 HF together with various catalysts and succeeded in the formation of monofluorinated alkenes.[57,66,68,69] Hammond reported on a gold-catalyzed hydrofluorination of alkynes to yield olefins with DMPU/HF as well as with pyridine·(HF)$_x$.[59,70] Moreover, the synthesis of β-fluorovinyl sulfones was studied by the group of Fustero, using copper-based catalysts together with Et$_3$N/HF.[60] Conversions in the presence of Lewis acids were reported by O'Hagan for hydrofluorinations of alkynyl sulfides using Et$_3$N·HF as HF source and TiF$_4$ or BF$_3$·Et$_2$O as Lewis acids.[71] Thibaudeau demonstrated the applicability of the superacid HF-SbF$_5$ in the hydrofluorination of ynamides at low temperatures, but it turned out that using pure anhydrous HF gave better yields.[72] Finally, a stable ion exchange resin loaded with anhydrous HF reagent was developed by Hammond, allowing for a hydrofluorination of alkenes and functionalized alkynes and ring-opening of aziridines.[73,74]

The ACF-loaded HF was tested in the hydrofluorination reactions of alkynes at 70 °C, and the reactions were monitored over seven days (Scheme 2). As shown in Scheme 3, in all cases, the fluorination occurred to give the Markownikow product. A second hydrofluorination was observed in certain cases, and fluorination takes place at the already fluorinated carbon. However, in comparison to other catalytic systems, such as the Au complex catalyzed DMPU/HF fluorination by Hammond et al., the conversions are low. They also reported for the same olefin that on using only fluorinating reagents, such as pyridine·(HF)$_x$, DMPU/HF, or even Bu$_4$N$^+$OTf$^-$/HF, no conversion was observed.[59,75]

It should be mentioned that in a comparable case, the reactivity of HF-loaded aluminium alkoxide fluoride was found to be significantly reduced compared to *high surface*-AlF$_3$ (*HS*-AlF$_3$).[32] Indeed, when this material was tested in the isomerization reaction of 1,2-dibromohexafluoropropane and in the dismutation reaction of dichlorodifluoromethane, no conversions at all were observed for both reactions, even when the temperature was increased up to 250 °C.[32] Those reactions can be usually performed at room temperature, by *HS*-AlF$_3$ or ACF, reaching 99 % conversion.[9]
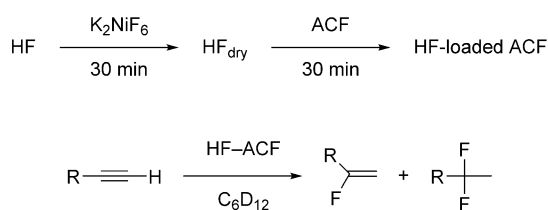
Scheme 2. Synthesis (up) and reactivity (bottom) of HF-loaded-ACF.
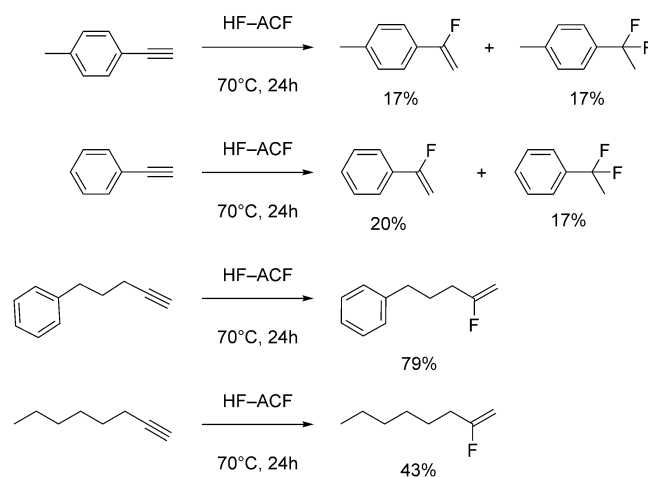
Scheme 3. Reactivity of various alkynes in the presence of HF-loaded-ACF.

Conclusions

HF was successfully immobilized at the surface of the ACF, by forming polyfluoride structures. The Lewis and Brønsted acidity are strongly reduced, presumably due to the interactions with surface Lewis sites as well as with surface fluorides. Thus, loading HF at the surface of ACF does not result in the generation of a superacid similar to systems such as SbF$_5$/HF. Comparable observations were reported by Kemnitz et al. for a compound with HF immobilized at aluminium alkoxide fluoride.[32] MAS NMR and X-ray data of HF-loaded ACF indicate a slight reorganization of the bulk. Heating leads to fluorination and crystallization processes, which might even already be initiated at room temperature. This would also result in a reduced Lewis-acidity. The loaded HF can further be transferred to alkynes by hydrofluorination under mild conditions to yield fluorinated alkenes, which are currently of interest as fluorinated building blocks.[76–78]

Experimental Section

General procedures

ACF was synthesized according to the literature.[13] HF (gift from Solvay Fluor GmbH) was dried using potassium hexafluoronickelate prior to the loading onto the surface of ACF.[79] In a flow of an argon stream, HF was condensed onto the drying agent, forming a deep red solution. The dry HF was then condensed onto 3 g of ACF for 30 minutes, and the excess of HF was then removed under vacuum. Before and after the loading with HF, the material was weighted and an increase of about 8 % in weight was observed for the loaded sample.

A second batch of HF-loaded ACF was synthesized, in the same way, as described, but a smaller amount of pre-dried HF was condensed onto the surface of ACF to obtain an HF moistened ACF.

CAUTION! Appropriate safety precautions must be taken when using HF, which is a highly toxic and irritant compound. Severe burns can be caused if HF comes in contact with the skin.

MAS NMR spectroscopy

The MAS NMR spectra were recorded on a Bruker AVANCE 600 spectrometer ($B_0 = 14.1$ T) at room temperature using a 2.5 mm magic angle sample spinning (MAS) probe and the MAS frequency was 27.5 kHz. The spectra shown in Figure 5, 6 and in the Supporting Information were recorded on a Bruker AVANCE 400 spectrometer ($B_0 = 9.4$ T) at room temperature, using the same 2.5 mm rotor. The rotation frequency used was 20 kHz. The chemical shifts are given with respect to (i) the $CFCl_3$ standard for ^{19}F, (ii) TMS for ^1H, and (iii) and aqueous solution of $AlCl_3$ for ^{27}Al. Data analysis was performed with the software TopSpin 2.1.

FTIR/INS

All FTIR spectra were acquired with a Bruker Vertex 70 spectrometer equipped with an ATR unit (diamond). Inelastic neutron scattering spectra were collected on the indirect geometry instrument TOSCA[80,81] at the ISIS Neutron and Muon Facility. Samples (0.928 g HF-loaded ACF) were loaded under argon atmosphere into Al sachets and sealed into Al sample holders before loading onto the instrument. The samples were cooled to < 20 K prior to data collection in order to minimize Debye-Waller dampening. Data were collected in the forward and backwards scattering geometries and summed.

Thermoanalysis

The thermal behavior of the solids was studied by conventional thermal analysis (TA) in an argon atmosphere. A NETZSCH Thermo analyzer STA409C Skimmer, being additionally equipped with a conventional high-temperature SiC oven, was used to record the thermoanalytical curves. An online-coupled BALZERS QMG 421 enabled MS-analysis of evolved gases. A DTA-TG sample carrier system with platinum crucibles (beaker, 0.8 mL) and Pt/PtRh10 thermocouples were used. Measurements were performed under an argon atmosphere by applying a heating rate of 10 K min^{-1}.

XRD

X-ray powder diffraction measurements were performed on an STOE Stadi MP diffractometer equipped with a Dectris Mythen 1 K linear silicon strip detector and Ge(111) double-crystal monochromator (Mo-Kα_1 radiation) in a transmission geometry.

Surface area determination and pore size analysis

The porosity of materials was measured by nitrogen adsorption–desorption using an Autosorb iQ instrument with Helium mode. Brunauer–Emmett–Teller (BET) surface area (SBET) was calculated in relative pressure range (p/p_0) from 0.05 to 0.35. Pore size distribution was calculated using the NLDFT Model.[82]

CD$_3$CN and pyridine adsorption followed by DRIFTS measurements

Diffuse reflectance infrared Fourier transform spectra (DRIFTS) of adsorbed deuterated acetonitrile (CD$_3$CN) were measured using a PIKE Technologies DiffusIR Environmental chamber (HTV) and DiffusIR diffuse reflectance accessory. Prior to the measurements, the samples were kept under vacuum for 2 h, then contacted with 90 mbar of CD$_3$CN or pyridine, and afterward degassed for 30 min at room temperature. All spectra were recorded on a Thermo Fischer Scientific Nicolet iS50 spectrometer equipped with an MCT

detector at 2 cm^{-1} spectral resolution over the range 4000–600 cm^{-1}.

Reactivity towards alkynes

All the reactions were performed using a Glovebox or conventional Schlenk techniques. C_6D_{12} was purchased from Eurisotop and dried over molecular sieves and purged by bubbling argon prior to use. The substrates were purchased from Sigma Aldrich and employed without further purification. A PTFE inliner was loaded with 25 mg of HF-loaded ACF inside a Glove-box and put in a closed JYoung NMR tube. The alkynes (0.3 mmol) were added together with C_6D_{12} as a solvent (0.4 mL) under Schlenk conditions in the PTFE inliner. The tubes were heated at 70 °C and reactions were monitored by ^1H and ^{19}F NMR spectroscopy over 7 days. The yields were calculated based on the amount of product by the integration of the ^{19}F NMR spectrum by using an external standard in a closed capillary (PhCF$_3$).

Conflict of interest

The authors declare no conflict of interest.

Keywords: aluminium · HF chemistry · hydrofluorination · metal fluorides

[1] C. Ni, J. Hu, *Chem. Soc. Rev.* **2016**, *45*, 5441–5454.
[2] K. Reichenbächer, H. I. Süss, J. Hulliger, *Chem. Soc. Rev.* **2005**, *34*, 22–30.
[3] D. O'Hagan, *Chem. Soc. Rev.* **2008**, *37*, 308–319.
[4] W. R. Dolbier, *J. Fluor. Chem.* **2005**, *126*, 157–163.
[5] T. Nakajima, B. Žemva, A. Tressaud, *Advanced Inorganic Fluorides: Synthesis Characterization, and Applications*, Elsevier, Berlin, **2000**.
[6] D. O'Hagan, D. B. Harper, *J. Fluor. Chem.* **1999**, *100*, 127–133.
[7] J. Wang, M. Sánchez-Roselló, J. L. Aceña, C. del Pozo, A. E. Sorochinsky, S. Fustero, V. A. Soloshonok, H. Liu, *Chem. Rev.* **2014**, *114*, 2432–2506.
[8] E. P. Gillis, K. J. Eastman, M. D. Hill, D. J. Donnelly, N. A. Meanwell, *J. Med. Chem.* **2015**, *58*, 8315–8359.
[9] T. Krahl, E. Kemnitz, *Catal. Sci. Technol.* **2017**, *7*, 773–796.
[10] E. Kemnitz, U. Groß, S. Rüdiger, C. S. Shekar, *Angew. Chem. Int. Ed.* **2003**, *42*, 4251–4254; *Angew. Chem.* **2003**, *115*, 4383–4386.
[11] T. Skapin, G. Tavčar, A. Benčan, Z. Mazej, *J. Fluor. Chem.* **2009**, *130*, 1086–1092.
[12] A. C. Sievert, C. G. Krespan, F. J. Weigert, *Process for Chlorofluoropropanes*, US5157171A.
[13] T. Krahl, E. Kemnitz, *J. Fluor. Chem.* **2006**, *127*, 663–678.
[14] T. Krahl, R. Stösser, E. Kemnitz, G. Scholz, M. Feist, G. Silly, J. Y. Buzaré, *Inorg. Chem.* **2003**, *42*, 6474–6483.

Chemistry–A European Journal

Full Paper
doi.org/10.1002/chem.202001627

Chemistry Europe
European Chemical
Societies Publishing

[15] B. Calvo, J. Wuttke, T. Braun, E. Kemnitz, *ChemCatChem* **2016**, *8*, 1945–1950.

[16] M. Ahrens, G. Scholz, T. Braun, E. Kemnitz, *Angew. Chem. Int. Ed.* **2013**, *52*, 5328–5332; *Angew. Chem.* **2013**, *125*, 5436–5440.

[17] G. Meißner, D. Dirican, C. Jäger, T. Braun, E. Kemnitz, *Catal. Sci. Technol.* **2017**, *7*, 3348–3354.

[18] T. Braun, F. Wehmeier, K. Altenhöner, *Angew. Chem. Int. Ed.* **2007**, *46*, 5321–5324; *Angew. Chem.* **2007**, *119*, 5415–5418.

[19] B. Calvo, C. P. Marshall, T. Krahl, J. Kröhnert, A. Trunschke, G. Scholz, T. Braun, E. Kemnitz, *Dalt. Trans.* **2018**, *47*, 16461–16473.

[20] B. Calvo, T. Braun, E. Kemnitz, *ChemCatChem* **2018**, *10*, 403–406.

[21] M.-C. Kervarec, C. P. Marshall, T. Braun, E. Kemnitz, *J. Fluor. Chem.* **2019**, *221*, 61–65.

[22] J. K. Murthy, U. Gross, S. Rüdiger, V. V. Rao, V. V. Kumar, A. Wander, C. L. Bailey, N. M. Harrison, E. Kemnitz, *J. Phys. Chem. B* **2006**, *110*, 8314–8319.

[23] M. H. G. Prechtl, M. Teltewskoi, A. Dimitrov, E. Kemnitz, T. Braun, *Chem. Eur. J.* **2011**, *17*, 14385–14388.

[24] M. Feist, M. Ahrens, A. Siwek, T. Braun, E. Kemnitz, *J. Therm. Anal. Calorim.* **2015**, *121*, 929–935.

[25] G. Meißner, K. Kretschmar, T. Braun, E. Kemnitz, *Angew. Chem. Int. Ed.* **2017**, *56*, 16338–16341; *Angew. Chem.* **2017**, *129*, 16556–16559.

[26] A. K. Siwek, M. Ahrens, M. Feist, T. Braun, E. Kemnitz, *ChemCatChem* **2017**, *9*, 839–845.

[27] V. A. A. Petrov, C. G. G. Krespan, B. E. E. Smart, *J. Fluorine Chem.* **1996**, *77*, 139–142.

[28] V. A. Petrov, C. G. Krespan, B. E. Smart, *J. Fluorine Chem.* **1998**, *89*, 125–130.

[29] C. G. Krespan, D. A. Dixon, *J. Fluorine Chem.* **1996**, *77*, 117–126.

[30] G. Meißner, M. Feist, T. Braun, E. Kemnitz, *J. Organomet. Chem.* **2017**, *847*, 234–241.

[31] C. L. Bailey, A. Wander, S. Mukhopadhyay, B. G. Searle, N. M. Harrison, *Phys. Chem. Chem. Phys.* **2008**, *10*, 2918.

[32] S. K. Ruediger, U. Groß, M. Feist, H. A. Prescott, S. C. Shekar, S. I. Troyanov, E. Kemnitz, *J. Mater. Chem.* **2005**, *15*, 588–597.

[33] I. G. Shenderovich, S. N. Smirnov, G. S. Denisov, V. A. Gindin, N. S. Golubev, A. Dunger, R. Reibke, S. Kirpekar, O. L. Malkina, H.-H. Limbach, *Ber. Bunsenges. Phys. Chemie* **1998**, *102*, 422–428.

[34] L. Gouin, J. Cousseau, J. A. S. Smith, *J. Chem. Soc. Faraday Trans. 2* **1977**, *73*, 1878–1883.

[35] R. König, G. Scholz, R. Bertram, E. Kemnitz, *J. Fluorine Chem.* **2008**, *129*, 598–606.

[36] R. König, G. Scholz, E. Kemnitz, *J. Sol.-Gel Sci. Technol.* **2010**, *56*, 145–156.

[37] R. König, G. Scholz, K. Scheurell, D. Heidemann, I. Buchem, W. E. S. Unger, E. Kemnitz, *J. Fluorine Chem.* **2010**, *131*, 91–97.

[38] H. Baumgarth, G. Meier, T. Braun, B. Braun-Cula, *Eur. J. Inorg. Chem.* **2016**, 4565–4572.

[39] K. M. Harmon, R. R. Lovelace, *J. Phys. Chem.* **1982**, *86*, 900–903.

[40] U. Gross, S. Rüdiger, E. Kemnitz, K. W. Brzezinka, S. Mukhopadhyay, C. Bailey, A. Wander, N. Harrison, *J. Phys. Chem. A* **2007**, *111*, 5813–5819.

[41] B. Desbat, P. V. Huong, *J. Chem. Phys.* **1983**, *78*, 6377–6383.

[42] S. Hirata, S. Iwata, *J. Phys. Chem. A* **1998**, *102*, 8426–8436.

[43] T. Nakajima, B. Žemva, A. Tressaud, *Advanced Inorganic Fluorides: Synthesis, Characterization and Applications*, Elsevier, Amsterdam, **2000**.

[44] A. Ažman, A. Ocvirk, D. Hadži, P. A. Giguère, M. Schneider, *Can. J. Chem.* **1967**, *45*, 1347–1350.

[45] T. von Rosenvinge, M. Parrinello, M. L. Klein, *J. Chem. Phys.* **1997**, *107*, 8012–8019.

[46] E. Kemnitz, S. Coman, *New Mater. Catal. Appl.*, Elsevier, **2016**, pp. 133–191.

[47] E. Kemnitz, D.-H. H. Menz, *Prog. Solid State Chem.* **1998**, *26*, 97–153.

[48] G. B. McVicker, C. J. Kim, J. J. Eggert, *J. Catal.* **1983**, *80*, 315–327.

[49] N. Herron, W. E. Farneth, *Adv. Mater.* **1996**, *8*, 959–968.

[50] J. A. Ibers, *J. Chem. Phys.* **1964**, *40*, 402–404.

[51] Z. Kaawar, B. Paulus, *J. Fluor. Chem.* **2019**, *224*, 67–72.

[52] B. A. Coyle, L. W. Schroeder, J. A. Ibers, *J. Solid State Chem.* **1970**, *1*, 386–393.

[53] E. P. Parry, *J. Catal.* **1963**, *2*, 371–379.

[54] A. Platon, W. J. Thomson, *Ind. Eng. Chem. Res.* **2003**, *42*, 5988–5992.

[55] I. Nastova, T. Skapin, L. Pejov, *Surf. Sci.* **2011**, *605*, 1525–1536.

[56] F. Nahra, S. R. Patrick, D. Bello, M. Brill, A. Obled, D. B. Cordes, A. M. Z. Slawin, D. O'Hagan, S. P. Nolan, *ChemCatChem* **2015**, *7*, 240–244.

[57] T. J. O'Connor, F. D. Toste, *ACS Catal.* **2018**, *8*, 5947–5951.

[58] R. Gauthier, M. Mamone, J. F. Paquin, *Org. Lett.* **2019**, *21*, 9024–9027.

[59] O. E. Okoromoba, J. Han, G. B. Hammond, B. Xu, *J. Am. Chem. Soc.* **2014**, *136*, 14381–14384.

[60] R. Román, P. Barrio, N. Mateu, D. M. Sedgwick, S. Fustero, *Molecules* **2019**, *24*, 1569.

[61] D. M. Sedgwick, I. López, R. Román, N. Kobayashi, O. E. Okoromoba, B. Xu, G. B. Hammond, P. Barrio, S. Fustero, *Org. Lett.* **2018**, *20*, 2338–2341.

[62] G. A. Olah, J. T. Welch, Y. D. Vankar, M. Nojima, I. Kerekes, J. A. Olah, *J. Org. Chem.* **1979**, *44*, 3872–3881.

[63] C. Hollingworth, V. Gouverneur, *Chem. Commun.* **2012**, *48*, 2929.

[64] G. A. Olah, X.-Y. Li, *Synlett* **1990**, 267–269.

[65] G. A. Olah, X.-Y. Li, Q. Wang, G. K. S. Prakash, *Across Conventional Lines: Selected Papers of George A. Olah, Vol.* 2 (Eds: G. A. Olah, G. K. S. Prakash), World Scientific, Singapore, **2003**, pp. 1020–1026.

[66] J. A. Akana, K. X. Bhattacharyya, P. Müller, J. P. Sadighi, *J. Am. Chem. Soc.* **2007**, *129*, 7736–7737.

[67] G. He, S. Qiu, H. Huang, G. Zhu, D. Zhang, R. Zhang, H. Zhu, *Org. Lett.* **2016**, *18*, 1856–1859.

[68] B. C. Gorske, C. T. Mbofana, S. J. Miller, *Org. Lett.* **2009**, *11*, 4318–4321.

[69] A. Gómez-Herrera, F. Nahra, M. Brill, S. P. Nolan, C. S. J. Cazin, *ChemCatChem* **2016**, *8*, 3381–3388.

[70] X. Zeng, S. Liu, G. B. Hammond, B. Xu, *Chem. Eur. J.* **2017**, *23*, 11977–11981.

[71] D. Bello, D. O'Hagan, *Beilstein J. Org. Chem.* **2015**, *11*, 1902–1909.

[72] G. Compain, K. Jouvin, A. Martin-Mingot, G. Evano, J. Marrot, S. Thibaudeau, *Chem. Commun.* **2012**, *48*, 5196.

[73] Z. Lu, B. S. Bajwa, O. E. Otome, G. B. Hammond, B. Xu, *Green Chem.* **2019**, *21*, 2224–2228.

[74] Z. Lu, B. S. Bajwa, S. Liu, S. Lee, G. B. Hammond, B. Xu, *Green Chem.* **2019**, *21*, 1467–1471.

[75] O. E. Okoromba, *Development and Applications of Novel HF-Based Fluorination Reagents: DMPU-HF*, PhD Thesis, University of Louisville, **2016**.

[76] M. J. Koh, T. T. Nguyen, H. Zhang, R. R. Schrock, A. H. Hoveyda, *Nature* **2016**, *531*, 459–465.

[77] J.-F. Nadon, K. Rochon, S. Grastilleur, G. Langlois, T. T. H. Dao, V. Blais, B. Guérin, L. Gendron, Y. L. Dory, *ACS Chem. Neurosci.* **2017**, *8*, 40–49.

[78] P. B. Huleatt, M. L. Khoo, Y. Y. Chua, T. W. Tan, R. S. Liew, B. Balogh, R. Deme, F. Gölöncsér, K. Magyar, D. P. Sheela, H. K. Ho, B. Sperlágh, P. Mátyus, C. L. L. Chai, *J. Med. Chem.* **2015**, *58*, 1400–1419.

[79] Z. Mazej, P. Benkič, A. Tressaud, B. Žemva, *Eur. J. Inorg. Chem.* **2004**, 1827–1834.

[80] S. F. Parker, F. Fernandez-Alonso, A. J. Ramirez-Cuesta, J. Tomkinson, S. Rudic, R. S. Pinna, G. Gorini, J. Fernández Castañon, *J. Phys. Conf. Ser.* **2014**, *554*, 012003.

[81] R. S. Pinna, S. Rudić, S. F. Parker, J. Armstrong, M. Zanetti, G. Škoro, S. P. Waller, D. Zacek, C. A. Smith, M. J. Capstick, D. J. McPhail, D. E. Pooley, G. D. Howells, G. Gorini, F. Fernandez-Alonso, *Nucl. Instruments Methods Phys. Res. Sect. A Accel. Spectrometers Detect. Assoc. Equip.* **2018**, *896*, 68–74.

[82] J. Landers, G. Y. Gor, A. V. Neimark, *Colloids Surf. A* **2013**, *437*, 3–32.